

Parallax in microlensing toward the Magellanic Clouds: impact on detection efficiency and detectability

T. Blaineau¹, M. Moniez¹

Laboratoire de physique des 2 infinis Irène Joliot-Curie, CNRS Université Paris-Saclay, Bât. 100, Faculté des sciences, F-91405 Orsay Cedex, France

Received 06/06/2019, accepted xx/xx/xxxx

ABSTRACT

Aims. We study the impact of the parallax on the search for very long timescale microlensing events towards the Magellanic Clouds due to dark massive compact objects within the past MACHO and EROS, the on-going MOA and OGLE, and the future LSST surveys. We quantify the impact of neglecting this effect on the classical event selection process and also quantify the parallax detectability without the help of follow-up observations.

Methods. We define a distance between true events affected by parallax and the closest events without parallax. This distance is used to estimate the probability of missing the preselection of events because of parallax, for any survey characterised by its time sampling and photometric performance. We also define another distance to quantify the detectability of the parallax effect, in order to trigger complementary observations.

Results. We find that the preselection of years long time scale events is marginally affected by parallax for all surveys, provided the criteria are reasonably tight. We also show that the parallax should be detectable in the majority of the events found by the LSST survey without follow-up observations.

Key words. Gravitational lensing: micro - surveys - stars: black hole - Galaxy: halo - Galaxy: kinematics and dynamics - Cosmology: dark matter

1. Introduction

The recently observed gravitational waves (Abbott et al. 2016a,b) can be emitted by possible candidates for the Galactic halo dark matter (Bird et al. 2016). The quest for direct evidence of intermediate mass black holes has resulted in a revival of the long time-scale microlensing searches (more than a few years). After Paczyński's publication (Paczynski (1986)) several teams – EROS (Expérience de Recherche d'Objets Sombres, Aubourg et al. (1993)), MACHO (MAssive Compact Halo Objects, Alcock et al. (1993)), OGLE (Optical Gravitational Lensing Experiment, Udalski et al. (1993)) and MOA (Microlensing Observations in Astrophysics, Sako et al. (2007)) – have operated systematic microlensing survey programs to search for hidden massive compact objects. The global result is that objects lighter than $10M_{\odot}$ contribute for a negligible fraction of the Galactic spherical halo mass. Searches are now underway to explore the halo beyond this limit, by searching for longer time scale events either by combining the databases (MEMO project, Mirhosseini & Moniez (2018)), by extending the surveys (OGLE), or by optimizing the strategy of the LSST (Large Synoptic Survey Telescope) forthcoming survey.

In this letter, we examine one specificity of the long time scale events, which is the distortions expected from the orbital motion of Earth around the Sun (so-called parallax effect in this paper), that can become significant for events longer than a few months.

Send offprint requests to: M. Moniez,
e-mail: moniez@1a1.in2p3.fr

In Sect. 2 we compare a microlensing event as seen from the Sun and the Earth. In Sect. 3, we describe a procedure to simulate a representative sample of microlensing events – taking into account parallax – as expected from Galactic hidden massive compact objects distributions. In Sect. 4 we propose a quantitative characterization of the distortion induced by the parallax with respect to the simple, rectilinear motion events. We deduce the maximum impact on the microlensing first level filtering, tuned by considering only non-parallax events. In Sect. 5, we define a proxy of the significance of parallax, that can be used for any microlensing survey. We evaluate the parallax detectability from simple representations of surveys, based on the time sampling and the photometric resolution in two realistic cases: the MEMO and the LSST projects (Sect. 6).

In this paper, we focus on the microlensing detection towards the Magellanic Clouds (LMC, SMC), where the dark matter signal from compact objects is expected mainly from a distribution model between a spherical halo and a thick disk.

2. The microlensing effect and the parallax

Microlensing occurs when a massive compact object passes close enough to the line of sight of a background source, temporarily magnifying its brightness. A review of the microlensing formalism can be found in Schneider et al. (2006) and Rahvar (2015). When a single point-like lens of mass M located at distance D_L deflects the light from a point source located at distance D_S , the magnification $A(t)$ of the source luminosity is given by

(Paczynski (1986))

$$A(t) = \frac{u(t)^2 + 2}{u(t) \sqrt{u(t)^2 + 4}}, \quad (1)$$

where $u(t)$ is the distance of the lensing object to the undeflected line of sight, divided by the Einstein radius r_E :

$$r_E = \sqrt{\frac{4GM}{c^2} D_S x(1-x)} \simeq 4.54 \text{ AU} \left[\frac{M}{M_\odot} \right]^{\frac{1}{2}} \left[\frac{D_S}{10 \text{ kpc}} \right]^{\frac{1}{2}} \frac{[x(1-x)]^{\frac{1}{2}}}{0.5}. \quad (2)$$

Here G is the Newtonian gravitational constant, and $x = D_L/D_S$. If the lens moves at a constant relative transverse velocity v_T , and $u(t)$ reaches its minimum value u_0 (impact parameter) to the undeflected line of sight at time t_0 , then $u(t) = \sqrt{u_0^2 + (t - t_0)^2/t_E^2}$, where $t_E = r_E/v_T$ is the lensing timescale:

$$t_E \sim 79 \text{ days} \times \left[\frac{v_T}{100 \text{ km/s}} \right]^{-1} \left[\frac{M}{M_\odot} \right]^{\frac{1}{2}} \left[\frac{D_S}{10 \text{ kpc}} \right]^{\frac{1}{2}} \frac{[x(1-x)]^{\frac{1}{2}}}{0.5}. \quad (3)$$

v_T is a combination of the source, lens, and observer velocities. If the microlensing is observed from the Sun, v_T is a constant, but if it is observed from the Earth, v_T includes a rotating component, responsible for the so-called parallax effect.

2.1. Microlensing events observed from the Sun

The so-called simple (or standard) microlensing effect (point-like source and lens with rectilinear motions) has the following characteristic features: the event is singular in the history of the source (as well as in the history of the deflector); the magnification $A(t)$ does not depend of the color, and is a function of time depending only on (u_0, t_0, t_E) , with a symmetric shape; the prior distribution of the events' impact parameters u_0 is uniform; all stars at the same given distance have the same probability of being lensed.

This simple microlensing description can be altered by many different effects: for example by parallax, multiple lens and source systems (Mao & Di Stefano (1995)), extended sources (Yoo et al. (2004))...

2.2. Microlensing events observed from the Earth

The orbital motion of Earth induces a curved (non rectilinear) relative motion of the deflector with respect to the line of sight (Gould (1992)). Figure 1 shows the configuration of a microlensing event as seen from the source, projected in the transverse plane containing the Sun. To take into account the parallax, two extra parameters are needed:

- $\pi_E = \frac{r_\oplus}{r_E}(1-x)$: the ratio between the Earth orbital radius and the projected Einstein radius.
- $\theta \in [0, 2\pi]$: the angle between \mathbf{i} , and the deflector's transverse speed vector (see Fig. 1).

Since the invariance of a microlensing event with respect to the lens moving direction is broken, we account for this by allowing u_0 taking negative value when the kinetic momentum $\mathbf{u}_D(t) \wedge \mathbf{v}_D$ is opposite to \mathbf{k} . The reference time t_0 is now the time of minimum approach of the deflector to the line of sight from the Sun (*n.b.* not the Earth). The positions of the projections of the

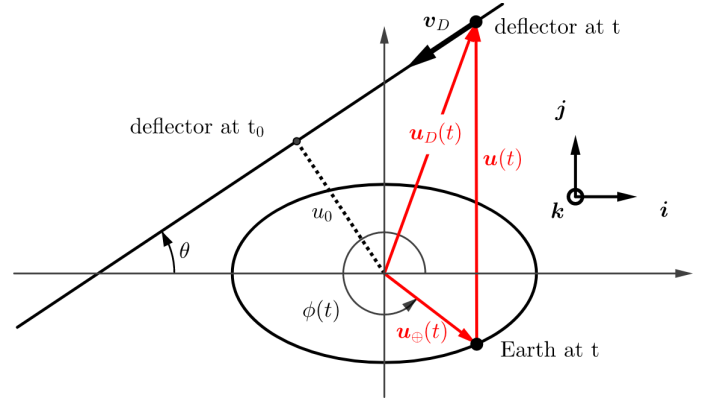


Fig. 1: *Parallax in microlensing. Projection from the source (here in the northern ecliptic hemisphere) on the plane (\mathbf{i} , \mathbf{j}), perpendicular to the Sun-source direction \mathbf{k} containing the Sun. \mathbf{i} is along the intersection of the ecliptic and transverse planes, its orientation is such that the perpendicular projection of \mathbf{j} on the ecliptic plane is opposite to the source.*

Earth and the deflector in the $(\mathbf{i}, \mathbf{j}, \mathbf{k})$ frame are expressed in unit of projected Einstein radius $r_E/(1-x)$ as:

$$\mathbf{u}_\oplus(t) = \begin{bmatrix} \pi_E \cos \phi(t) \\ \pi_E \sin \phi(t) \sin \beta_\star \\ 0 \end{bmatrix}, \mathbf{u}_D(t) = \begin{bmatrix} -u_0 \sin \theta - \frac{t-t_0}{t_E} \cos \theta \\ u_0 \cos \theta - \frac{t-t_0}{t_E} \sin \theta \\ 0 \end{bmatrix}, \quad (4)$$

where $\phi(t)$ is defined on Fig. 1, and β_\star is the ecliptic latitude of the source star, hence the angle between the Ecliptic plane and the plane transverse to the line of sight. The impact parameter from Earth is therefore given by $u(t) = \|\mathbf{u}_D(t) - \mathbf{u}_\oplus(t)\|$.

3. Simulation of microlensing parameters

To study the effect of parallax in detecting microlensing events, we generate microlensing parameters from dark matter distribution models (spherical halo and thick disk). To be as general as possible, we consider only the magnifications and do not simulate measures specific to one survey, avoiding extensive experiment simulation of time sampling, photometric errors... These characteristics of the surveys will be taken into account independently in an approximate way further in this paper.

We considered the two simple lenses distributions used in many microlensing surveys analyses: a galactic spherical halo model and a dark matter thick disk. These models correspond to two extreme lens distance distributions, from nearby to widely distributed lens distances.

3.1. Spherical halo

The spherical halo model consists in a spherical, isotropic, isothermal dark matter halo distribution. The mass spatial distribution is given by:

$$\rho(r) = \rho_\odot \frac{R_c^2 + R_\odot^2}{r^2 + R_c^2}, \quad (5)$$

where $R_c = 5 \text{ kpc}$ is the "core" radius of the galaxy, $R_\odot = 8.5 \text{ kpc}$ is the distance from the Sun to the Galactic Center (GC), $\rho_\odot = 0.0079 M_\odot \text{ pc}^{-3}$ is the local dark matter density and r is

the distance from the GC. The lens velocity vector (\mathbf{v}) orientations are uniformly distributed while the velocity norm probability distribution is:

$$p(v) = 4\pi v^2 \left(\frac{1}{2\pi v_0^2} \right)^{3/2} e^{-\frac{v^2}{2v_0^2}} \quad (6)$$

where the velocity dispersion is $v_0 = 120 \text{ km s}^{-1}$ (Battaglia et al. (2005)).

3.2. Thick disk

We also considered a dark matter thick disk model (from Rahal et al. (2009) with mass density

$$\rho_{TD}(r, z) = \frac{\Sigma}{2H} \exp\left(-\frac{r-R_\odot}{R}\right) \exp\left(-\frac{|z|}{H}\right). \quad (7)$$

We set the column density at $\Sigma = 35 M_\odot \text{ pc}^{-2}$, the height scale at $H = 1.0 \text{ kpc}$, and the radial length scale at $R = 3.5 \text{ kpc}$. The velocity of a thick disk object can be decomposed into two components: the global rotation speed, to which is added a peculiar velocity. The global disk rotation velocity depends on the distance r from the GC in the cylindrical galactocentric system:

$$\mathbf{v}_{\text{rot}}(r) = -v_{\text{rot},\odot} \left[1.00767 \left(\frac{r}{R_\odot} \right)^{0.0394} + 0.00712 \right] \mathbf{u}_\theta, \quad (8)$$

where $v_{\text{rot},\odot} = 239 \text{ km s}^{-1}$ is the global rotation speed at the Sun position (Brunthaler et al. (2011)). The peculiar velocity distribution is described by an anisotropic gaussian distribution characterized by the following radial, tangential and perpendicular velocity dispersions (Pasetto et al. (2012)):

$$(\sigma_r, \sigma_\theta, \sigma_z) = (56.1 \pm 3.8, 46.1 \pm 6.7, 35.1 \pm 3.4) \text{ km s}^{-1} \quad (9)$$

3.3. Common parameters

The galactocentric coordinates¹ of the LMC global velocity vector are (Kallivayalil et al. (2013)):

$$\mathbf{v}_{LMC} = (-57, -226, 221)_{\text{XYZ}} \text{ km s}^{-1}, \quad (10)$$

The Sun velocity vector is the sum of the global Galactic rotation component and the peculiar velocity component (Brunthaler et al. (2011)):

$$\mathbf{v}_\odot = (11.1, 12.24 + v_{\text{rot},\odot}, 7.25)_{\text{XYZ}} \text{ km s}^{-1}. \quad (11)$$

We simulate microlensing for 6 masses: 0.1, 1, 10, 30, 100 and 300 M_\odot .

From the generated physical values we can compute the magnification curve parameters x , t_E , π_E and θ . u_0 and t_0 are then generated uniformly ($u_0 \in [-2, 2]$, t_0 spanning all seasons). We do not simulate blending (but see the discussion section). Since we only care about the magnification, we do not consider the source fluxes, and assume that fluxes are measured with the nominal photometric precision for each survey. We generated a few million of parameter sets for lenses belonging to each dark matter structure, spherical halo and thick disk. Splitting the samples into two halves, we checked that the results from each subsample are compatible, confirming that this statistics is not limiting. Since we do not simulate light curves as obtained from a given survey, we define in the next sections metrics only taking the microlensing event parameters as input.

¹ The origin is the GC, \mathbf{X} points from the Sun toward the GC, \mathbf{Y} points in the same direction than the Sun velocity vector, \mathbf{Z} points toward the Galactic North Pole (Gardiner et al. (1994)).

4. The impact of parallax on the event detection

Parallax can sometimes significantly distort a microlensing event lightcurve by making it asymmetric and/or multi-peaked with approximately yearly gaps. Before discussing the impact of these distortions, we briefly remind the philosophy of the historical microlensing searches: the detection of events results from a preselection based on loose selection cuts, requesting a single bump in the light-curve, with little constraint on the shape. Usually, microlensing events are then identified through visual control within this sample, which is much wider than the final selection. After this preselection, an automatic (blind) selection is applied using tighter criteria on the shape of the light-curve (such as χ^2 of a simple microlensing fit), in order to optimise the rejection of artefacts to microlensing. At this level, genuine microlensing events identified during the preselection maybe rejected because of parallax distortions. Such an automatic selection is necessary to compute a detection efficiency, needed for optical depth² and event rate measurements.

That said, several effects from the parallax distortions have to be distinguished:

- *Detection of events*: Here, the question is to quantify the probability to miss good S/N events during the preselection, because of parallax.
- *Detection efficiency*: The complete automatic selection is obviously more sensitive to the shape of the events, and the selected event counts used in the efficiency computing may be affected by the parallax.

To study the perturbation to the *detection of events*, we quantify the impact of the parallax using a metric (distance function) between theoretical parallax and standard event light-curves, and the count of peaks in the light-curves.

4.1. Minimal absolute photometric difference D_π

In most cases, even if the light curve seen from the Earth differs significantly from the one seen from the Sun, its shape remains almost identical to a standard light curve, but with different parameters. To quantify the light-curve shape distortion, our metric is computed from the *closest* simple microlensing event magnitude light-curve $m_\odot(t, t_E, t_0, u_0)$ to the considered parallax event $m_\oplus(t)$ by minimizing the maximum absolute difference:

$$D_\pi = \min_{t_E, t_0, u_0} \left\{ \max_t |m_\oplus(t) - m_\odot(t, t_E, t_0, u_0)| \right\}. \quad (12)$$

4.2. Number of peaks

The microlensing surveys usually include in the prefiltering the condition of observing only one significant peak. Thus, in addition to D_π , we compute the number of distinct peaks exhibited by the parallax light curve. A peak is defined by an interval during which the amplification exceeds a given threshold (depending on the survey). We estimate the number of peaks in measured light-curves assuming a daily sampling rate, which is better than all the past and planned cadencing, thus providing conservative upper numbers of peaks.

² The optical depth is the probability for a given line-of sight to intercept a deflector's Einstein disk.

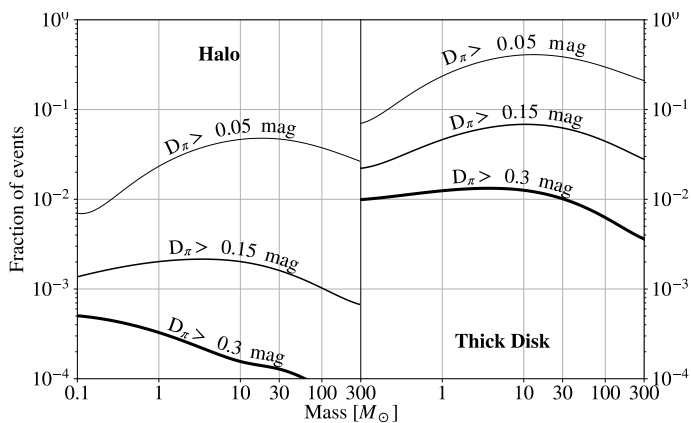


Fig. 2: Fraction of light-curves with best fitted (simple event) $u_0 < 1$. and D_π larger than (0.05, 0.15, 0.3) magnitude, as a function of the deflectors' mass. Spherical halo dark matter model (left); thick disk dark matter model (right).

4.3. Quantifying the probability to miss events

We only consider events with an "effective" fitted impact parameter³ $|u_0| < 1$, as most research algorithms require a minimum magnification of 1.34, corresponding to $u = 1$ in Eq. (1).

Figure 2 shows the fraction of events with D_π larger than given thresholds (0.05, 0.15, 0.3 magnitudes), as a function of the deflectors' mass. The curves corresponding to $D_\pi > 0.05$ mag. are the easiest to interpret, since 0.05 mag. (chosen to be conservative) corresponds to the typical best photometric resolution σ_{phot} of the historical surveys (EROS, MACHO, MOA, OGLE2-3). We can read from Fig. 2 that a maximum of 5% (resp. 40%) of the event light-curves from the halo dark matter model (resp. thick disk) can deviate by more than 0.05 magnitudes from a standard microlensing light-curve. This means that at least 95% (resp. 60%) of the events are indistinguishable from standard events as soon as $\sigma_{\text{phot}} > 0.05$. The fraction of events deviating by more than 0.15 magnitudes is always smaller than 1% for objects from the halo dark matter model, and less than 8% for the thick disk dark matter model.

Let's have a closer look on the case of events due to lenses belonging to the thick disk dark matter model, where deviations can be somewhat more frequent (max. 40% with $D_\pi > 0.05$ mag., max. 8% with $D_\pi > 0.15$ mag.). We estimate that the probability to find more than one peak above any threshold comprised between 0.05 and 0.5 magnitude during the pre-filtering process is negligible (less than 0.6% for thick disk events and even less for halo events). Since a common pre-filtering requirement is the presence of only one significant bump along the light curve, this means that no event from lenses between 0.1 to 300 M_\odot should be eliminated by this requirement, which is insensitive to the precise shape of the bump.

The first (conservative) conclusion is that if lenses belong to a halo, the pre-filtering of microlensing events should never miss more than 5% of the long events because of the parallax; if lenses belong to a thick disk, the distortions may more frequently exceed 0.05 magnitude. Nevertheless, since the usual pre-filtering tolerates a shape alteration less than 0.15 mag., and since there is no more than one peak in the light-curve, such a pre-filtering should not miss more than 8% of the long events.

Regarding the automatic selection algorithm efficiency, it appears that as soon as a criterion for the goodness of the fit is used,

³ u_0 of the best simple microlensing curve associated to D_π .

it has to either be loose enough to allow for ~ 0.15 magnitude variations (case of thick disk lenses) or be estimated taking into account parallax. In the case of a sub-percent photometric survey like LSST, the automatic detection efficiency needed to estimate the microlensing optical depth or to establish limits on the thick disk contribution to dark matter will need to properly account for parallax, and more specific studies will be necessary.

5. Potential of parallax detection

In the previous section, we discussed the impact of parallax on the detection of microlensing events; in this section, we discuss the probability to detect the parallax in addition to the microlensing effect. Such a detection offers the potential to significantly improve the constraints on the microlensing event configurations (Gould (1992)). Moreover a systematic search for parallax during on-going events enables the possibility to trigger complementary fast sampled, multi-color or any other specific observations.

5.1. Minimal integral photometric difference

To get an estimate of the proportion of events with detectable parallax effect, we quantify the parallax significance with a pseudo- χ^2 defined as:

$$\tilde{\chi}_\pi^2 = N_{\text{obs}} + \frac{f_s}{\sigma_{\text{phot}}^2} \min_{t_E, t_0, u_0} \int_{-\infty}^{+\infty} (m_\odot(t, t_E, t_0, u_0) - m_\oplus(t))^2 dt \quad (13)$$

where m_\odot (resp. m_\oplus) is the lensed source magnification function seen from the Sun (resp. from Earth), and f_s –the sampling frequency–, σ_{phot} –the mean photometric error– and $N_{\text{obs}} = T_{\text{obs}} \times f_s$ –the number of measures–, characterize the survey. This pseudo- χ^2 is a proxy of the χ^2 of the best standard microlensing fit to an hypothetical observed light curve containing N_{obs} observations, sampling a true microlensing light-curve $m_\oplus(t)$ (with parallax), with a constant photometric precision σ_{phot} .

Yet obviously $\tilde{\chi}_\pi^2$ cannot account for all subtleties of a dedicated simulation as:

- This quantity does not take into account variations of the photometric precision with the magnitude or with the observational conditions. As a consequence, this pseudo- χ^2 is an averaged proxy.
- For simplicity, the integral is extended to infinity instead of the time interval of observation T_{obs} . This approximation is pessimistic, since events with parallax deviations exceeding T_{obs} interval will have a larger $\tilde{\chi}_\pi^2$ than when restricting the integral to T_{obs} .
- Time sampling is more critical for short and/or highly magnified events. This is why we will trust this proxy mainly for long time-scale event studies; the exact time distribution of the measurements should not significantly impact parallax detection for several years long events, provided that there are no year-long gaps without measurements.

After minimizing the integral from Eq. (13) we can compute $\tilde{\chi}_\pi^2$ by setting the parameters N_{obs} (or T_{obs}), f_s and σ_{phot} associated to a given survey. From $\tilde{\chi}_\pi^2$, we compute an associated significance of the improvement from standard fit to a parallax fit (in σ) and estimate the fraction of events with detectable parallax effect (at 3σ and 5σ).

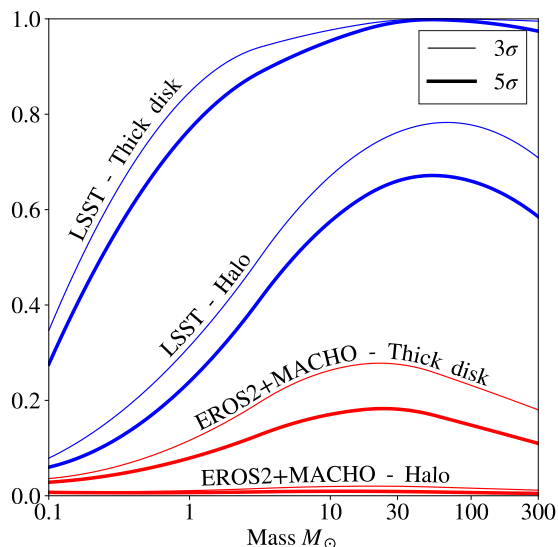


Fig. 3: Fraction of events with parallax significance larger than 3σ (thin lines) and 5σ (thick lines), as a function of the lens mass.

5.2. Quantifying the parallax detectability

Using the optimal parameters for the joint EROS2+MACHO surveys ($\sigma_{phot.} = 0.05$ mag, $f_s = 0.2$ day $^{-1}$, $T_{obs} = 4000$ days), and the projected parameters for LSST ($\sigma_{phot.} = 0.005$ mag, $f_s = 0.25$ day $^{-1}$, $T_{obs} = 4000$ days), we obtain the curves shown in Fig. 3 for 3σ and 5σ detection. Regarding the dark matter spherical halo model, we expect a negligible fraction of events to have a significant parallax signature in the combined database of EROS2 and MACHO; conversely, LSST alone (*i.e.* with no follow-up observations) should be able to detect parallax of more than 65% of the microlensing events in a $10 M_{\odot}$ - $300 M_{\odot}$ mass range, due to a greatly improved photometric precision. If we consider a dark matter thick disk model, the fraction of events with a measurable parallax effect is significant in both surveys (except for $0.1 M_{\odot}$ deflectors for EROS2+MACHO). The high sensitivity to parallax found for the LSST case is in good agreement with a previous study (Rahvar, S. et al. (2003)) assuming Hubble Space Telescope observations triggered by Earth microlensing alert systems.

6. Discussion

In this study, we have neglected the cases of other non-standard microlensing effects (multiple sources and structured lenses), which represents a marginal statistics.

We checked the robustness of our conclusions with respect to blending: the catalogued sources in the microlensing surveys are frequently composite objects; in such a situation, the observed light-curves is the superposition of a microlensing light-curve and a constant one. We have simulated parallaxed events with up to a 50% blend contribution to the light-curve and have considered the same ratios as defined in Fig. 2. We find that, at least up to a 50% blending level, the probability to miss events when ignoring the parallax is only marginally changed with respect to the no blend case.

Our study focus on the case of dark matter black holes belonging to a spherical halo or a thick disk. Any other reasonable dark matter structure model, like flattened halo model, should have a lens distance distribution and kinematical data that are

comprised between these two limiting cases. Therefore the numbers extracted from Figs. 2 and 3 provide minimum and maximum fractions of events. The conclusions relative to the impact on the prefiltering may thus be generalized to other halo models, and the expected fractions of detectable parallax events should be interpolated between those extreme values. We plan to deliver the results of an equivalent study for the microlensing searches towards the galactic plane in a forthcoming paper.

7. Conclusions and perspectives

Our study shows that parallax has a negligible effect on prefiltering of long duration (more than a few months) microlensing events toward LMC/SMC in the case of either a dark matter spherical halo or a dark matter thick disk composed of black holes. But parallax should be taken into account for computing the efficiency of automatic filtering algorithms, specifically for the next-generation experiments with sub-percent level of photometric accuracy; dedicated simulation based on realised observation cadences and observations will be necessary to precisely assess this detection efficiency to extract optical depths and event rates. On another note, for the majority of lenses with mass larger than $10 M_{\odot}$ toward LMC/SMC, LSST-like surveys should be able to detect and quantify the parallax, allowing better determination of the lensing configuration parameters, and a discrimination between the dark matter structure models.

Acknowledgements. We thank Olivier Perdereau and Sylvie Dagoret-Campagne for their useful comments on the manuscript. This work was supported by the Paris Ile-de-France Region.

References

- Abbott, B., Abbott, R., Abbott, T., et al. 2016a, Phys. Rev. Lett., 116, 241103
- Abbott, B., Abbott, R., Abbott, T., et al. 2016b, Phys. Rev. Lett., 116, 061102
- Alcock, C., Akerlof, C., Allsman, R., et al. 1993, Nature, 365
- Aubourg, E., Baryre, P., Bréhin, S., et al. 1993, Nature, 365, 623
- Battaglia, G., Helmi, A., Morrison, H., et al. 2005, MNRAS, 364, 433
- Bird, S., Cholis, I., Muñoz, J. B., et al. 2016, Phys. Rev. Lett., 116, 201301
- Brunthaler, A., Reid, M. J., Menten, K. M., et al. 2011, Astronomische Nachrichten, 332, 461
- Gardiner, L. T., Sawa, T., & Fujimoto, M. 1994, MNRAS, 266, 567
- Gould, A. 1992, ApJ, 392, 442
- Kallivayalil, N., van der Marel, R. P., Besla, G., Anderson, J., & Alcock, C. 2013, ApJ, 764, 161
- Mao, S. & Di Stefano, R. 1995, ApJ, 440, 22
- Mirhosseini, A. & Moniez, M. 2018, A&A, 618, L4
- Paczynski, B. 1986, ApJ, 304, 1
- Pasetto, S., Grebel, E. K., Zwitter, T., et al. 2012, A&A, 547, A70
- Rahal, Y. R., Afonso, C., Albert, J. N., et al. 2009, A&A, 500, 1027
- Rahvar, S. 2015, International Journal of Modern Physics D, 24, 1530020
- Rahvar, S., Moniez, M., Ansari, R., & Perdereau, O. 2003, A&A, 412, 81
- Sako, T., Sekiguchi, T., Sasaki, M., et al. 2007, Experimental Astronomy, 22, 51–66
- Schneider, P., Kochanek, C., & Wambsganss, J. 2006, Gravitational Lensing: Strong, Weak and Micro
- Udalski, A., Szymanski, M., Kaluzny, J., et al. 1993, Acta Astron., 43, 289
- Yoo, J., DePoy, D. L., Gal-Yam, A., et al. 2004, ApJ, 603, 139